Slave-boson study of the t-t'-J model: Phase diagram, spin susceptibility, and Hall resistivity

M. Deeg and H. Fehske
Physikalisches Institut, Universität Bayreuth, D-95440 Bayreuth, Germany
(Received 20 June 1994)

We investigate the normal-state properties of high-T_c cuprates in terms of the t-t'-J model using a spin-rotation-invariant slave-boson technique. The second-neighbor hopping $t'<0$ is included in order to reproduce the Fermi surfaces of LSCO ($La_{2-x}Sr_xCuO_4$) and YBCO ($YBa_2Cu_3O_{6+x}$) type. The magnetic phase diagram of the t-t'-J model is derived within the saddle-point approximation, by taking into account also incommensurate spiral order. Compared to the pure t-J model, Néel order is stabilized in the low-doping region. In particular, for the case $t'>0$, which corresponds to the electron-doped systems, e.g., $Nd_{2-x}Ce_xCuO_4$ (NCCO), the antiferromagnetic correlations are strongly enhanced near half-filling. We include fluctuation corrections and calculate the dynamic (paramagnetic) spin susceptibility $\chi(\mathbf{q},\omega)$ going beyond the random-phase approximation. The instability line of the paraphase obtained from $\chi(\mathbf{q})$ is in agreement with the saddle-point phase diagram. The wave-vector dependence of $\chi(\mathbf{q})$ reveals the commensurate (incommensurate) nature of spin fluctuations in YBCO (LSCO). Finally, the doping dependence of the Hall resistivity $R_H(\delta)$ is calculated, where the results agree surprisingly well with experiments on LSCO. For YBCO and NCCO, the t' term suffices to give the correct dependence for $R_H(\delta)$.

One of the remarkable differences between $La_{2-x}Sr_xCuO_4$ (LSCO) and $YBa_2Cu_3O_{6+x}$ (YBCO) types of high-T_c cuprates is the nature of spin excitations in the metallic phase probed by inelastic neutron scattering[1] and nuclear magnetic resonance/nuclear quadrupole resonance (NMR/NQR) relaxation[2] experiments. In the LSCO family, incommensurate peaks [around $(\pi(1\pm q_0),\pi)$, $(\pi,\pi(1\pm q_0))$, for $q_0(x)$, see Ref. 3] have been reported in the dynamic structure factor $S(\mathbf{q},\omega)$, whereas, upon doping, $S(\mathbf{q},\omega)$ keeps its commensurate maximum at (π,π) for the YBCO system. The physical origin of the contrasting $\mathbf{q}$ depending of the spin fluctuation spectrum is still under discussion. Millis and Monien[4] have argued that the spin dynamics and, in particular, the temperature dependence of spin susceptibility $\chi_s(T)$ in LSCO are caused by a spin-density wave instability, whereas in the YBCO family they are due to in-plane antiferromagnetic (AFM) fluctuations and a non-Fermi-liquid spin singlet pairing of electrons in adjacent planes. On the other hand, the magnetic properties are intimately related to the energy-band dispersion of the noninteracting system within a Fermi-liquid-based framework, i.e., in this way the observed spin dynamics can be attributed to different Fermi-surface (FS) geometry of LSCO type and YBCO type, respectively. Along this line, details of the spin fluctuation spectrum are studied using a nearly antiferromagnetic Fermi-liquid approach by Monthoux and Pines[5] and within a large Coulomb-U auxiliary boson scheme by Si *et al.*[6] It is interesting to note that a simple band-structure model of LSCO together with marginal-Fermi-liquid self-energy corrections,[7] i.e., without strong AFM exchange enhancement as in the models,[5,6] can give an energy and momentum dependence of the magnetic structure factor in parallel to Refs. 5 and 6. Therefore Littlewood *et al.*[7] are lead to the conclusion that the peaks seen in neutron scattering derive primarily from FS geometry. From a more microscopic point of view, the important effect of FS shape on the magnetic properties were confirmed by Kohno and coworkers[8] using a resonating valence band (RVB) slave-boson mean-field approach to the extended t-J model. Furthermore, Ito, Takenaka, and Uchida[9] have recently reported that the charge transport in the CuO_2 plane is determined by dominant spin scattering, i.e., the spin dynamics are manifest in the extraordinary transport properties of the high-T_c cuprates as well.

II. MODEL AND METHODOLOGY

Encouraged by these findings it is the aim of this paper to study magnetic and transport phenomena on an equal footing in terms of probably the most simple effective one-band model describing both different correlation and band-structure effects, the so-called t-t'-J model:

$$\mathcal{H}_{t\text{-}t'\text{-}J}=-t\sum_{\langle i,j\rangle,\sigma}\tilde{c}^{\dagger}_{i\sigma}\tilde{c}_{j\sigma}-t'\sum_{\langle\langle i,j\rangle\rangle,\sigma}\tilde{c}^{\dagger}_{i\sigma}\tilde{c}_{j\sigma}+J\sum_{\langle ij\rangle}\left(\mathbf{S}_i\cdot\mathbf{S}_j-\frac{n_in_j}{4}\right). \tag{1}$$

$\mathcal{H}_{t\text{-}t'\text{-}J}$ acts in a projected Hilbert space without double occupancy, where $\tilde{c}^{(\dagger)}_{i\sigma}=c^{(\dagger)}_{i\sigma}(1-n_{i-\sigma})$ is the electron annihilation (creation) operator, $\mathbf{S}_i=\frac{1}{2}\sum_{\sigma\sigma'}\tilde{c}^{\dagger}_{i\sigma}\tau_{\sigma\sigma'}\tilde{c}_{i\sigma'}$, $n_i=n_{i\uparrow}+n_{i\downarrow}$, and $n_{i\sigma}=\tilde{c}^{\dagger}_{i\sigma}\tilde{c}_{i\sigma}$. J measures the AFM exchange interaction, t and t' denote hopping processes between nearest-neighbor (NN pairs: $\langle i,j\rangle$) and next-nearest-neighbor (NNN pairs: $\langle\langle i,j\rangle\rangle$) sites on a square lattice. Compared to the original t-J model the t' term incorporates several important effects near half-filling. Starting from a rather complex two-band model for the

CuO_2 planes, quantum cluster calculations[10] have revealed that the relative large direct transfer between NN oxygen sites ($t_{pp} \lesssim t_{pd}/2$) leads to a sizable NNN hopping t' in the context of an effective one-band description. More recently the t' term has been introduced to reproduce the FS geometry observed in angle-resolved photoemission spectroscopy experiments (in the noninteracting limit).[8,11–13] Fitting the quasiparticle dispersion relation

$$\varepsilon_{\mathbf{k}} = -2t(\cos k_x + \cos k_y) - 4t' \cos k_x \cos k_y \ , \tag{2}$$

involved in (1), to experimental and band-theory results yields t in the order of 0.3 eV and, e.g., for the case of YBCO, $t' \simeq -0.4t$.[5,6,14] Moreover, Tohyama and Maekawa[13] have emphasized that a t-t'-J model with $t'>0$ can be used to describe the electron-doped systems, e.g., $Nd_{2-x}Ce_xCuO_4$ (NCCO). In this case one has to shift the momentum $\mathbf{k} \rightarrow \mathbf{k}+(\pi,\pi)$,[13] i.e., within a band-filling scenario one obtains a hole pocket like FS centered at the (π,π) point which *shrinks* with increasing doping.[15] Finally, as pointed out by Lee,[16] in a local AFM environment a hole can propagate coherently only on the same sublattice without disturbing spins. Therefore the t' term coupling the same sublattice becomes crucial for the low-lying magnetic excitations. This clearly is a correlation effect related to the NNN hopping processes.

To proceed we apply to $\mathcal{H}_{t\text{-}t'\text{-}J}$ a [SU(2)⊗U(1)] spin-rotation-invariant slave-boson (SB) scheme[17] based on the SB approach developed for the Hubbard model by Kotliar and Ruckenstein[18] and Li, Wölfe, and Hirschfeld.[19] Our SB technique[17] provides an adequate description of spin and charge degrees of freedom by introducing auxiliary boson fields $e_i^{(\dagger)}$ and matrix operators $\underline{p}_i^{(\dagger)}$ (with scalar $p_0^{(\dagger)}$ and vector components $\mathbf{p}^{(\dagger)}$), representing empty and single occupied sites, respectively. Then the electronic (annihilation) operators are given in terms of bosonic ($\underline{z}_i$) and pseudofermionic (f_i) operators: $\tilde{c}_{i\sigma} = \sum_\rho z_{i\sigma\rho} f_{i\rho}$ (here ρ and σ denote spin indices), where the $\underline{z}$ factors[17,20] yield a correlation-induced band renormalization. The interaction term is bosonized via $n_i = 2\,\mathrm{Tr}\underline{p}_i^\dagger \underline{p}_i$ and $\mathbf{S}_i = \mathrm{Tr}\underline{p}_i^\dagger \underline{\tau} \underline{p}_i$. Now the partition function can be expressed as a coherent-state path integral

$$Z = \int \mathcal{D}[\Phi^*,\Phi] e^{-\mathcal{S}_{\mathrm{eff}}} \tag{3}$$

over bosonic fields

$$\Phi_i(\tau) = (e_i, p_{i0}, \lambda_{i0}^{(2)}, \lambda_i^{(1)}; \mathbf{p}_i, \boldsymbol{\lambda}_i^{(2)}) \ , \tag{4}$$

where the bosonic and fermionic parts of the effective action $\mathcal{S}_{\mathrm{eff}} = \mathcal{S}_{\mathrm{eff}}^B + \mathcal{S}_{\mathrm{eff}}^F$ are given by

$$\mathcal{S}_{\mathrm{eff}}^B = \int_0^\beta d\tau \left\{ \sum_i [\, \lambda_i^{(1)} e_i^2 + (\lambda_i^{(1)} - \lambda_{i0}^{(2)})(p_{i0}^2 + \mathbf{p}_i^2) - 2p_{i0}\mathbf{p}_i \cdot \boldsymbol{\lambda}_i^{(2)} - \lambda_i^{(1)}] + J \sum_{\langle ij \rangle} [\, p_{i0}\mathbf{p}_i \cdot \mathbf{p}_j p_{j0} - \tfrac{1}{4}(p_{i0}^2 + \mathbf{p}_i^2)(p_{j0}^2 + \mathbf{p}_j^2)] \right\} , \tag{5}$$

and

$$\mathcal{S}_{\mathrm{eff}}^F = -\mathrm{Tr}_{ij,\tau\tau',\rho\rho'} \ln\{-G^{-1}_{ij,\rho\rho'}(\tau,\tau')\} \ , \tag{6}$$

$$G^{-1}_{ij,\rho\rho'}(\tau,\tau') = [(-\partial_\tau + \mu - \lambda_{i0}^{(2)})\delta_{\rho\rho'} - \boldsymbol{\lambda}_i^{(2)} \cdot \boldsymbol{\tau}_{\rho\rho'}] \times \delta_{ij}\delta(\tau-\tau') + t(\underline{z}_i^\dagger \underline{z}_j)_{\rho\rho',\tau\tau'}(1-\delta_{ij}) \ , \tag{7}$$

respectively. In contrast to the Hubbard model,[21] the radial gauge could be used to remove *all* phases of the Bose fields, i.e., the $\Phi_{i\alpha}(\tau)$ ($\alpha = 1, \ldots, 10$) become real.[17] In (3) five dynamic Lagrange-multiplier fields ($\lambda_i^{(1)}$, $\lambda_{i0}^{(2)}$, $\boldsymbol{\lambda}_i^{(2)}$) have been introduced to eliminate the unphysical states in the extended Hilbert space (*local* constraints). Let us emphasize that a spin-rotation-invariant bosonization of the t-t'-J model is necessary to guarantee that (i) the spin-algebra is satisfied and (ii) the SB Hamiltonian $\mathcal{H}_{t\text{-}t'\text{-}J}^{\mathrm{SB}}$ yields the same matrix elements as (1) in the physical subspace.

The evaluation of (3) proceeds via the saddle-point expansion, where at the first level of approximation we look for an extremum of the bosonized action $\mathcal{S}_{\mathrm{eff}}$ with respect to the boson fields and the Lagrange multipliers using the ansatz $\mathbf{m}_i \propto \mathbf{n}_i = (\cos\mathbf{Q}\mathbf{R}_i, \sin\mathbf{Q}\mathbf{R}_i, 0)$ for the local magnetization $\mathbf{m}_i = -2\mathbf{S}_i = -2p_{i0}\mathbf{p}_i$. Following earlier analyses of spiral states for the Hubbard model[22–24] the unit vector $\mathbf{n}_i$ is chosen as a local spin quantization axis pointing in opposite directions on different sublattices. Thereby, the "order parameter" wave vector $\mathbf{Q}$ is introduced to describe several magnetic ordered states: paramagnetic (PM), ferromagnetic (FM) ($\mathbf{Q}=0$), AFM [$\mathbf{Q}=(\pi,\pi)$], and incommensurate (1,1)-spiral [$\mathbf{Q}=(Q,Q)$], $(1,\pi)$-spiral [$\mathbf{Q}=(Q,\pi)$] and (0,1)-spiral [$\mathbf{Q}=(0,Q)$] states.

III. RESULTS

A. Magnetic phase diagram

Comparing the free energies of several (homogeneous) symmetry broken states, we obtain the SB phase diagram of the t-t'-J model shown as a function of hole doping ($\delta = 1-n$) in Fig. 1. In the numerical work, we take $J/t = 0.4$, which seems to be a realistic parameter for the

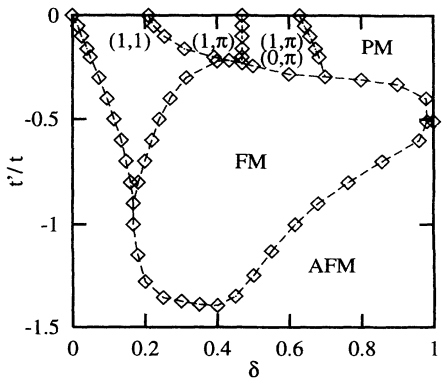

FIG. 1. Restricted ground-state phase diagram of the two-dimensional t-t'-J model at $J/t = 0.4$.

exchange interaction in both LSCO and YBCO (Refs. 12, 13, and 17) (within a strong-coupling expansion of the Hubbard model this corresponds to $U/t=10$). We can distinguish two regimes in the phase diagram. In the parameter regime $|t'/t| \lesssim 0.2$, Fig. 1 resembles the ground-state phase diagram of the t-J model obtained recently by us.[17] Especially we found large regions with incommensurate spiral magnetic order. However, compared to the pure t-J model, the t' term stabilizes Néel order in a finite δ region near half-filling. The increasing stability of AFM configurations can be intuitively understood because the t' term moves electrons without disturbing the Néel-like background.[13] For larger ratios $|t'/t|$ we have a completely different situation. In this parameter regime only commensurate states (AFM, FM, PM) occur, where for $t'<t'_c=-1.4t$ we obtain the AFM state for all δ. Note the rather large differences to the value of t'_c obtained within a semiclassical $(1/N)$ expansion.[25] By varying the exchange coupling J the phase boundaries in the $t'/t-\delta$ plane are not much affected, e.g., for $J/t=1$ and $t'/t=-0.4$, the transitions AFM$\rightleftarrows$(1,1)-spiral and (1,1)-spiral$\rightleftarrows$FM take place at $\delta=0.17$ and 0.6, respectively. We would like to point out here that the main *qualitative* features of our SB phase diagram confirm recent studies of magnetic long-range order in the t-t'-J model.[25,26]

Figure 2 displays the variation of the "extremal" wave vector as a function of doping at $t'/t=\pm 0.16$ and $t'/t=-0.4$. Usually the value $t'/t=-0.16$ (-0.4) is chosen to fit the band structure of the LSCO (YBCO) family.[8,11,12,24] In Fig. 2 a negative value of δ denotes the case of electron doping. The behavior of Q_x reflects a series of transitions AFM$\rightleftarrows$(1,1)-spiral$\rightleftarrows$(1,0)-spiral$\rightleftarrows$PM. The corresponding (sublattice) magnetization abruptly changes at the (1,1)-spiral$\rightleftarrows$(1,0)-spiral first-order transition. From Fig. 2 the asymmetry between hole $(t'<0)$ and electron doping $(t'>0)$ becomes evident. In contrast to recent Hartree-Fock results for the Hubbard model[24] we found the AFM phase near half-filling for both electron-doped and hole-doped cases (provided $t'\neq 0$). In the absence of t' hopping, for arbitrarily small doping, the AFM is found to be unstable against the (1,1)-spiral phase (cf. Fig. 1). Obviously, the AFM correlations are strongly enhanced by a positive t' term, which is also in qualitative agreement with exact diagonalization studies of the t-t'-J model[13] and confirms the experimental findings from the electron-doped system NCCO.[27] Note that the stability region of the AFM phase agrees surprisingly well with the combined phase diagram for $La_{2-x}Sr_xCuO_4$ and $Nd_{2-x}Sr_xCuO_4$ obtained from neutron scattering[28] and muon spin relaxation measurements,[29] respectively. For the YBCO parameter $t'/t=-0.4$, the AFM disappears around $\delta=0.1$ whereas in the phase diagram of YBCO, determined by neutron diffraction,[30] this transition takes place at about $x=0.4$ *oxygen* content. However, there exists strong evidence that at least up to $x=0.2$ *no holes* are transferred from Cu(1) to Cu(2) planes (cf. the discussion of Fig. 6 below).

As we have already noted, the phase diagram presented in Fig. 1 results from the relative stability of various *homogeneous* states. However, there are arguments for

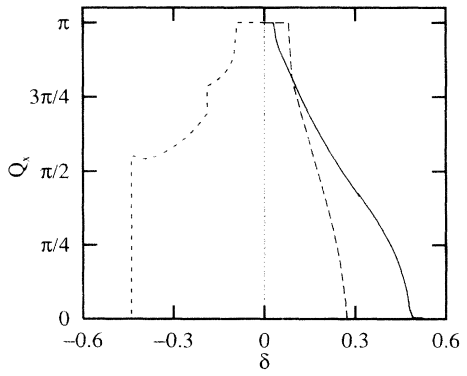

FIG. 2. The x component of the SB spiral wave vector $\mathbf{Q}$ away from half-filling for the negative values $t'/t=-0.16$ (solid line) and $t'/t=-0.4$ (long-dashed line), i.e., hole doping $(\delta>0)$, and for the positive one $t'/t=0.16$ (dashed line), i.e., electron doping $(\delta<0)$.

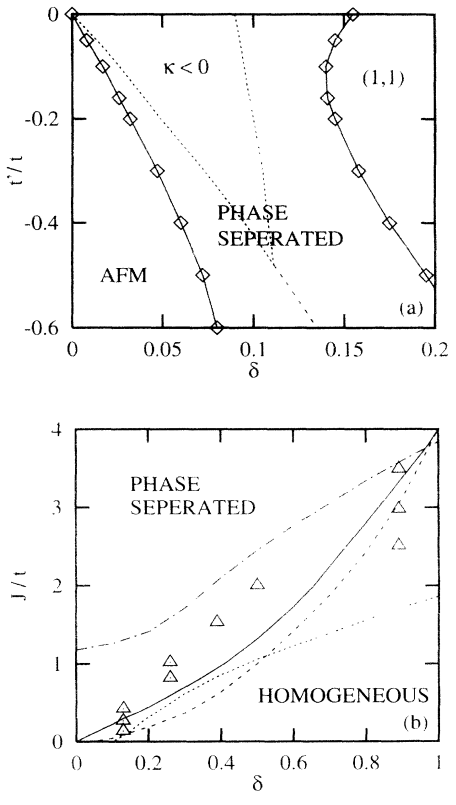

FIG. 3. The phase diagram of the t-t'-J model is calculated in the $t'/t-\delta$ plane at $J/t=0.4$ including phase separated states (a). The two-phase region consists of AFM and (1,1)-spiral states. Phase separation boundary (solid curve) for the pure t-J model in the J-δ plane (b). We include the transition lines of Ref. 34 (dashed), Ref. 36 (dotted), and Ref. 35 (dotted-dashed). The triangles are the Lanczos results of Ref. 32. For further explanation see text.

the existence of *inhomogeneous,* e.g., phase-separated states in the t-J and related models.[31] Using very different methods, it was realized by several groups,[32–36] that at large J/t the ground state of the t-J model separates into an AFM (hole-poor) and hole-rich region. Unfortunately, in the physically interesting regime of small exchange coupling ($J/t \sim 0.2$ to 0.4) and low-doping level this point is still controversial. To gain more insight about the phenomenon of phase separation in t-J-type models of strongly correlated electrons it seems to be important to investigate the effect of an additional NNN hopping term t' as well. Therefore we study the free energy as a function of hole density δ, where a (concave) convex curvature indicates local thermodynamic (in)stability [which implies a (negative) positive isothermal compressibility κ]. Then the domain of the two-phase regime is determined performing a Maxwell construction for the anomalous increase of the chemical potential μ with doping.[23] The results of our analysis of thermodynamic stability are depicted in Figs. 3(a) and 3(b) for the t-t'-J and t-J models, respectively. The dotted lines of zero inverse compressibility show that also for $|t'/t| > 0$ there is a finite range of δ over which the (1,1)-spiral is locally unstable. Similar results were recently obtained by Psaltakis and Papanicolaou.[25] It is important to stress that the AFM state is *locally* stable for *both* signs of t'. In addition, we demonstrate, based on the Maxwell construction, that near half-filling the AFM state remains also *globally* stable against phase separation [cf. Fig. 3(a), where the two-phase region is bounded by the solid lines]. At larger values of $|t'/t| \gtrsim 0.5$, the phase-separated region is due to the first-order nature of the transition AFM$\rightleftarrows$(1,1)-spiral (dashed curve).[25] At $t' \equiv 0$, i.e., for the pure t-J model, the boundary of phase separation is given in the J-δ plane by the solid curve shown in Fig. 3(b). Obviously, the homogeneous magnetic phases are always unstable close to half-filling (provided $J/t > 0$). This is in qualitative agreement with results obtained from exact diagonalization studies[32] as well as from semiclassical[34] or renormalization-group calculations.[36] Also plotted in Fig. 3(b) are the results of the high-temperature expansion method,[35] where phase separation may occur only above a critical exchange $J/t = 1.2$ as $\delta \rightarrow 0$, contrary to all the other approaches.

B. Spin susceptibility

In a next step we include quadratic terms (Gaussian fluctuations) in a fluctuation expansion ($\Phi_{i\alpha} = \bar{\Phi}_\alpha + \delta\Phi_{i\alpha}$) of the collective action

$$\mathcal{S}_{\text{Gauss}} = \bar{\mathcal{S}} + \sum_{q;\alpha,\beta} \delta\Phi_\alpha(-q)\mathcal{S}_{\alpha\beta}(q)\delta\Phi_\beta(q) \tag{8}$$

around the PM saddle-point solution $\{\bar{\mathcal{S}}, \bar{\Phi}_\alpha\}$. The paramagnetic spin susceptibility defined by

$$\chi_s = \sum_{\sigma\sigma'} \sigma\sigma' \langle \delta n_\sigma(-q)\delta n_{\sigma'}(q)\rangle$$

[or alternatively in functional integral representation by $\chi_s = 4\bar{\Phi}_2^2 \langle \delta\Phi_9(-q)\delta\Phi_9(q)\rangle$], can be expressed in terms of the inverse fluctuation propagator matrix as $\chi_s = 2p_0^2(\mathcal{S}^{-1})_{99}$ (cf. Refs. 37 and 38). From this we can derive the following expression for the dynamic spin susceptibility $\chi_s(q = (\mathbf{q}, i\omega_m))$ of the t-t'-J model:

$$\chi_s(q) = \frac{\bar{\chi}_0(q)}{1 + C(\mathbf{q})\bar{\chi}_0(q) + \mathcal{H}(q)} , \tag{9}$$

where

$$C(\mathbf{q}) = \frac{\delta}{(1+\delta)^3}[\bar{\varepsilon}(\mathbf{q}) + 3\bar{\varepsilon}(0)] + \frac{J(\mathbf{q})}{2} , \tag{10}$$

$$\mathcal{H}(q) = \frac{2\delta}{(1+\delta)^2}\bar{\chi}_1(q) + \frac{\delta^2}{(1+\delta)^4}[\bar{\chi}_1^2(q) - \bar{\chi}_0(q)\bar{\chi}_2(q)] , \tag{11}$$

$$\bar{\chi}_n(q) = -\frac{2}{\mathcal{N}} \sum_k (\varepsilon_{\mathbf{k}} + \varepsilon_{\mathbf{k}+\mathbf{q}})^n G(k)G(k+q) , \tag{12}$$

$J(\mathbf{q}) = J(\cos q_x + \cos q_y)$, and

$$\bar{\varepsilon}(\mathbf{q}) = \frac{2}{N} \sum_{\mathbf{k}} \varepsilon_{\mathbf{k}-\mathbf{q}}\theta[\tilde{\mu} - 2\varepsilon_{\mathbf{k}}\delta/(1+\delta)] .$$

Note that the Green propagators involved in (11) are dressed due to SB band renormalization, i.e.,

$$G(k) = [i\omega_n - 2\varepsilon_{\mathbf{k}}\delta/(1+\delta) + \tilde{\mu}]^{-1} ,$$

where $\tilde{\mu} = \mu - \lambda_0^{(2)}$ is the chemical potential. For the case $t' = 0$ (t-J model), a detailed numerical evaluation of the paramagnetic spin susceptibility for arbitrary frequencies, wave vectors, and band fillings were performed by Deeg *et al.*[38] Here we discuss the static susceptibility of the t-t'-J model. Then the instability line of the paramagnetic phase towards magnetic ordered states can be obtained analyzing the divergence (pole structure) of $\chi_s(\mathbf{q},0)$ as function of $\mathbf{q}$, δ, J/t, and t'/t. As shown in Fig. 4 for different ratios t'/t, the saddle-point phase boundary PM$\rightleftarrows$(1,π)/(0,π)-spiral (cf. Fig. 1) coincides with a divergence of $\chi_s((0,\pi),0)$ proving the consistency of both approaches. Obviously, the deviation of $\chi_s(q)$ from the standard random-phase approximation (RPA) form[8]

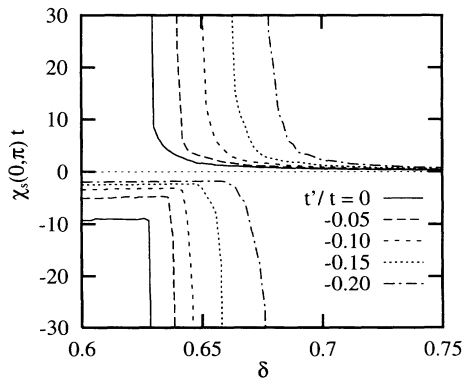

FIG. 4. Doping dependence of the static spin susceptibility $\chi((0,\pi),0)$ near the PM-$(0,\pi)$ spiral phase transition for $J/t = 0.4$ and different ratios t'/t.

$\chi_s(\mathbf{q},\omega)=\chi_0(\mathbf{q},\omega)/[1+J(\mathbf{q})\chi_0(\mathbf{q},\omega)]$ is necessary to reproduce the phase boundaries in the SB phase diagram. To elucidate the influence of t' on the detailed $\mathbf{q}$ dependence of the (generalized) polarization propagators $\bar{\chi}_n(\mathbf{q})$, in Fig. 5 we have plotted $\bar{\chi}_n(\mathbf{q})$ along the direction Γ-M-X-Γ in the square lattice Brillouin zone. For comparison with the results of Bénard, Chen, and Tremblay and Tanamoto, Kohno, and Fukuyama[8] we show $\bar{\chi}_n(\mathbf{q})$ for $\delta=0.1$, where in fact our theory yields magnetically ordered ground states (cf. Fig. 1). $\bar{\chi}_0(\mathbf{q})$ resembles the behavior of $\chi_0(\mathbf{q})$ used in previous RPA-like theories for the t-J (Ref. 8) and Hubbard models,[11,12] i.e., we observe (in)commensurate peak structures which can be attributed to FS effects (Kohn anomalies, cf. the discussion in Ref. 38). In the spinon-holon theory[8] the variation of $\chi_s(\mathbf{q})$ with respect to $\mathbf{q}$ is mainly governed by that of $\chi_0(\mathbf{q})$ and it is tempting to relate the structure of $\chi_s(\mathbf{q})$ around (π,π) to the magnetic peaks seen in neutron scattering data, i.e., the sharp incommensurate peaks for LSCO and the rather broad maximum for YBCO. Although to be fully consistent one has to calculate $\chi_s(\mathbf{q})$ also for the magnetically ordered phases, the behavior of the *paramagnetic* susceptibility can be taken as an indication that spiral states are good approximate candidates for the ground state of the t-t'-J model near half-filling.

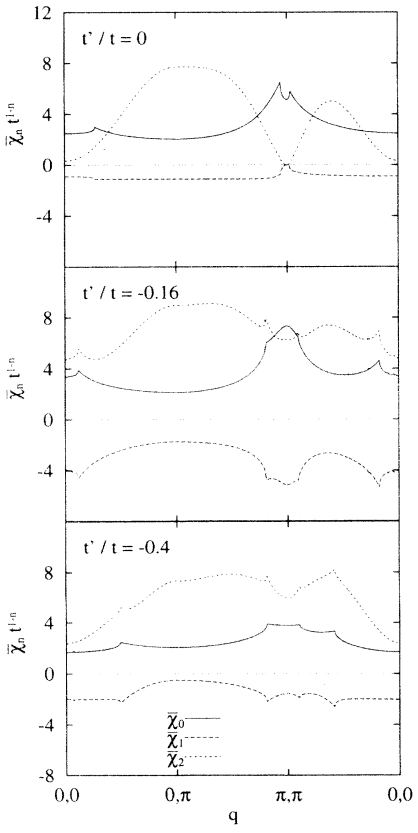

FIG. 5. Response functions $\bar{\chi}_n(\mathbf{q})$ along the highly symmetric directions of the Brillouin zone at doping level $\delta=0.1$.

The point we would like to emphasize here is the predominant role of $\bar{\chi}_1(\mathbf{q})$ and $\bar{\chi}_2(\mathbf{q})$ with increasing ratio $|t'/t|$. The higher-order Lindhard functions $\bar{\chi}_1(\mathbf{q})$ and $\bar{\chi}_2(\mathbf{q})$ differ in their $\mathbf{q},\omega$ dependence significantly from the ordinary Lindhard function. Recent work for the one-dimensional (1D) Hubbard model[39] shows the importance of these extended Lindhard functions for a consistent treatment of the dynamical charge correlations as well.

C. Hall resistivity

Finally, we turn to the calculation of the Hall resistivity $R_H=\sigma_{xyz}/\sigma_{xx}\sigma_{yy}$. Adopting the hypothesis of Trugman,[40] most of the normal-state properties can be explained by the dressing of quasiparticles due to magnetic interactions and the subsequent modification of their dispersion relation. Then, using the relaxation time approximation, the transport coefficients $\sigma_{\alpha\beta\gamma}$ and $\sigma_{\alpha\beta}$ are obtained by the standard Brillouin-zone integrals, where FS and correlation effects are involved via the renormalized SB quasiparticle band. With increasing $|t'/t|$, the correlation-induced band narrowing is weakened. Let us emphasize that in our approach the SB quasiparticle band is determined in a self-consistent way. This is in sharp contrast to the ($J=0$) SB mean field scheme of Chi and Nagi,[41] which results, in fact, in the simple replacement

$$\varepsilon_{\mathbf{k}}\rightarrow\tilde{\varepsilon}_{\mathbf{k}}=-2t\delta[(\cos k_x+\cos k_y)+2(t'/t)\cos k_x\cos k_y]$$

of the noninteracting band dispersion.

Figure 6 shows the theoretical Hall resistivity as function of carrier density in comparison to the experimental data for hole-doped systems LSCO (Ref. 42) and YBCO (Ref. 43) and for electron-doped compound NCCO.[44,45] For LSCO, the carrier density δ in the CuO_2 planes is definitively equal to the chemical composition x of Sr.[46] The NCCO system behaves quite similar, apart from the different sign of the carriers introduced by the substitution of Nd with Ce.[44] For YBCO, it seems to be more difficult to extract the number of holes from the experi-

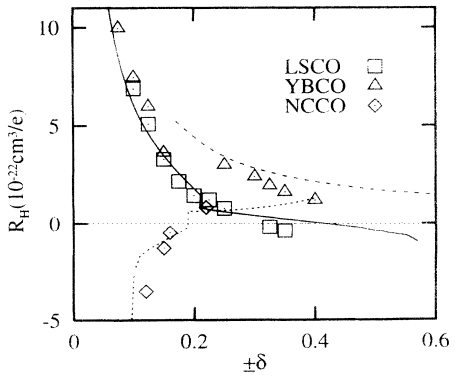

FIG. 6. Hall resistivity R_H vs doping δ for different values t'/t. Our SB results for $t'/t=0$ (solid), $t'/t=-0.4$ (dashed), and $t'/t=0.16$ (dotted) are compared with experiments on LSCO (Ref. 42), NCCO (Refs. 44 and 45) (at 80 K), and YBCO (Ref. 43) (at 100 K), respectively. The energy unit t is fixed to 0.3 eV and $J/t=0.4$.

mental data.[43] In order to compare our theoretical model with experiments on oxygen-doped YBCO,[43] we use the relation $\delta=(x-0.2)/2$ between transferred holes and oxygen content, in agreement also with recent suggestions by Rossat-Mignod *et al.*[30]

As can be seen from Fig. 6, the SB results are extremely sensitive to the choice of the NNN hopping parameter t'. For an exchange interaction strength $J/t=0.4$, a good agreement with experiments on LSCO and YBCO can be obtained using the (reasonable) parameter values $t'/t=0$ (Ref. 47) and $t'/t=-0.4$, respectively. For NCCO, the experimentally observed rapid decrease of the negative Hall coefficient $R_H(\delta)$ is clearly seen with decreasing δ [at electron doping level $\delta=-0.08$, we have $R_H^{\text{theory}}=-10.7$ compared to the experimental value $R_H^{\text{exp}}\simeq-8.2$ (Ref. 44) (in units of 10^{-22} cm$^3/e$)]. It is worth emphasizing that the low-temperature theoretical Hall resistivity is consistent with the experimental data for the hole (LSCO, YBCO) as well as for the electron-doped (NCCO) systems, including the sign change occuring at a very similar value, respectively. The temperature dependence of R_H will be presented together with a more detailed discussion of the correlation effects on the quasiparticle dispersion (Fermi surface) in a forthcoming paper.[48]

IV. SUMMARY

We have used a spin-rotation-invariant SB approach to investigate magnetic and transport properties of the 2D t-t'-J model. Our main results are the following.

(i) We present a detailed magnetic ground-state phase diagram of the 2D t-t'-J model, including incommensurate magnetic structures and phase separated states. At finite t', a main feature of the phase diagram, we would like to emphasize, is the existence of an AFM state away from half-filling, which is locally and also globally stable against phase separation. This result agrees with the experimentally observed persistence of finite range AFM order in the weakly doped LSCO and YBCO compounds. In contrast, for the simple t-J model we observe no AFM long-range order at any finite doping due to phase separation.

(ii) The next-nearest-neighbor hopping process (t') incorporates important correlation and band-structure effects near half-filling. In particular, the t' term can be used to reproduce the Fermi surfaces of LSCO, YBCO, and NCCO (in the noninteracting limit). Also the NNN hopping provides a possible origin for the experimentally observed asymmetry in the persistence of AFM long-range order of hole and electron-doped systems.

(iii) Including (Gaussian) fluctuations beyond the paramagnetic saddle-point approximation, we have derived a concise expression for the spin susceptibility $\chi_s(\mathbf{q},\omega)$ of the t-t'-J model, which does not have the standard RPA form. For $|t'/t|>0$, higher-order Lindhard functions are of increasing importance. The instability line obtained from a divergence of $\chi_s(\mathbf{q},0)$ is in agreement with the PM$\rightleftarrows$spiral-state phase boundary in the saddle-point phase diagram. The wave-vector dependence of $\chi_s(\mathbf{q},0)$ reveals the different nature of spin fluctuations reported by neutron-scattering experiments for LSCO and YBCO, respectively.

(iv) The doping dependence of the Hall resistivity shows the importance of both Fermi surface and correlation effects. Our slave-boson results for $R_H(\delta)$ agree even quantitatively with experiments on LSCO, YBCO, and NCCO.

ACKNOWLEDGMENT

The authors would like to thank K. Fesser for a critical reading of the manuscript.

[1] T. E. Mason, G. Aeppli, and H. A. Mook, Phys. Rev. Lett. **68**, 1414 (1992); J. Rossat-Mignod *et al.*, Physica C **185-189**, 86 (1991); M. Matsuda *et al.*, Phys. Rev. B **49**, 6958 (1994).

[2] H. Pennington and C. P. Slichter, *Physical Properties of High Temperature Superconductors* (World Scientific, Singapore, 1990), p. 269; F. C. Chou *et al.*, Phys. Rev. Lett. **71**, 2323 (1993).

[3] Y. Endoh *et al.*, Jpn. J. Appl. Phys. **7**, 174 (1992).

[4] A. J. Millis and H. Monien, Phys. Rev. Lett. **70**, 2810 (1993).

[5] P. Monthoux and D. Pines, Phys. Rev. B **49**, 4261 (1994).

[6] Q. Si, Y. Zha, K. Levin, and J. P. Lu, Phys. Rev. B **47**, 9055 (1993).

[7] P. Littlewood, J. Zaanen, G. Aeppli, and H. Monien, Phys. Rev. B **48**, 487 (1993).

[8] H. Kohno, T. Tanamoto, and H. Fukuyama, Physica B **186-188**, 941 (1991); T. Tanamoto, H. Kohno, and H. Fukuyama, J. Phys. Soc. Jpn. **62**, 717 (1993); **62**, 1455 (1993).

[9] T. Ito, K. Takenaka, and S. Uchida, Phys. Rev. Lett. **70**, 3995 (1993).

[10] M. S. Hybertsen, M. Schlüter, and N. E. Christensen, Phys. Rev. B **39**, 9028 (1989).

[11] P. Bénard, L. Chen, and A.-M. S. Tremblay, Phys. Rev. B **47**, 15 217 (1993).

[12] M. Lavagna and G. Stemmann, Phys. Rev. B **49**, 4235 (1994).

[13] T. Tohyama and S. Maekawa, Phys. Rev. B **49**, 3596 (1994).

[14] J. Yu, S. Massidda, and A. J. Freeman, Phys. Lett. A **122**, 198 (1987).

[15] D. M. King *et al.*, Phys. Rev. Lett. **70**, 3159 (1991); R. O. Anderson *et al.*, *ibid.* **70**, 3163 (1991).

[16] P. A. Lee, Phys. Rev. Lett. **63**, 680 (1989).

[17] M. Deeg, H. Fehske, and H. Büttner, Europhys. Lett. **26**, 109 (1994).

[18] G. Kotliar and A. E. Ruckenstein, Phys. Rev. Lett. **57**, 1362 (1986).

[19] T. Li, P. Wölfle, and P. J. Hirschfeld, Phys. Rev. B **40**, 6817 (1989).

[20] R. Frésard and P. Wölfle, Int. J. Mod. Phys. B **6**, 685 (1992); **6**, 3087(E) (1992).

[21] M. Deeg, H. Fehske, and H. Büttner, Z. Phys. B **88**, 283 (1992).

[22] R. Frésard, M. Dzierzawa, and P. Wölfle, Europhys. Lett. **15**, 325 (1991).

[23]E. Arrigoni and G. C. Strinati, Phys. Rev. B **44**, 7455 (1991).
[24]A. P. Kampf and W. Brenig, J. Low. Temp. Phys. **1/2**, 335 (1994).
[25]G. C. Psaltakis and N. Papanicolaou, Phys. Rev. B **48**, 456 (1993).
[26]H. Mori and M. Hamada, Phys. Rev. B **48**, 6242 (1993).
[27]V. Chechersky *et al.*, Phys. Rev. Lett. **70**, 3355 (1993); M. Matsuda *et al.*, Phys. Rev. B **45**, 12 548 (1992).
[28]G. M. Luke *et al.*, Phys. Rev. B **42**, 7981 (1990).
[29]T. R. Thurston *et al.*, Phys. Rev. B **40**, 4585 (1990).
[30]J. Rossat-Mignod *et al.*, Physica B **180&181**, 383 (1992).
[31]V. J. Emery and S. A. Kivelson, Physica C **209**, 597 (1993).
[32]V. J. Emery, S. A. Kivelson, and H. Q. Lin, Phys. Rev. Lett. **64**, 475 (1990); S. A. Kivelson, V. J. Emery, and H. Q. Lin, Phys. Rev. B **42**, 6562 (1990).
[33]H. Fehske *et al.*, Solid State Commun. **76**, 1333 (1990); Phys. Rev. B **44**, 8473 (1991); V. Waas, H. Fehske, and H. Büttner, *ibid.* **48**, 9106 (1993).
[34]M. Marder, N. Papanicolaou, and G. C. Pstaltakis, Phys. Rev. B **41**, 6920 (1990).
[35]W. O. Puttika, M. U. Luchini, and T. M. Rice, Phys. Rev. Lett. **68**, 538 (1992).
[36]E. V. L. de Mello, J. Phys. Condens. Matter **6**, 117 (1994).
[37]T. Li, Y. S. Sun, and P. Wölfle, Z. Phys. B **82**, 369 (1991).
[38]M. Deeg *et al.*, Z. Phys. B **95**, 87 (1994).
[39]T. Li, Phys. Rev. B **46**, 9301 (1992).
[40]S. A. Trugman, Phys. Rev. Lett. **65**, 500 (1990).
[41]H. Chi and A. D. S. Nagi, Phys. Rev. B **46**, 421 (1992).
[42]H. Takagi *et al.*, Phys. Rev. B **40**, 2254 (1989).
[43]E. Jones *et al.*, Phys. Rev. B **47**, 8986 (1993).
[44]H. Tagaki, S. Uchida, and Y. Tokura, Phys. Rev. Lett. **62**, 1197 (1989).
[45]S. J. Hagen, J. L. Peng, Z. Y. Li, and R. L. Greene, Phys. Rev. B **43**, 13 606 (1991).
[46]S. Uchida, Physica C **185-189**, 28 (1991).
[47]G. Dopf, A. Muramatsu, and W. Hanke, Phys. Rev. Lett. **68**, 353 (1992); note that their comparison of quantum Monte Carlo results for the three-band Hubbard model with experiments on LSCO leads to a parameter set, where the direct oxygen transfer (related to t' in our model) is equal to zero.
[48]H. Fehske and M. Deeg, Solid State Commun. **93**, 41 (1995).